Photonic Integrated Circuits: a Study on Process Variations

Mahdi Nikdast[1,2*], **Gabriela Nicolescu**[1], **Jelena Trajkovic**[3], **Odile Liboiron-Ladouceur**[2]
[1]*CE Dep., Polytechnique Montreal, Montreal, Canada* [2]*ECE Dep., McGill University, Montreal, Canada*
[3]*ECE Dep., Concordia University, Montreal, Canada*
mnikdast@ieee.org

Abstract: Developing an efficient method and applying it to study several identical microresonators fabricated by electron beam lithography, we quantify the worst-case within-die silicon thickness and resonance wavelength variations to be 1.55 and 2.11 nm, respectively.

OCIS codes: 250.5300, 200.4650.

1. Introduction

Designing silicon photonic integrated circuits (PICs) for wavelength-division multiplexing (WDM)-based applications requires a careful consideration of process variations. The functionality of such systems is highly tied to how well different devices are matched in terms of their central wavelengths. Some efforts have been made to characterize process variations in PICs [1–4], in which within-die, within-wafer, and wafer-to-wafer variations have been explored. Also, the silicon thickness variation is identified as the major concern. This paper presents a systematic perspective through developing a computationally efficient method to study the impact of process variations on large-scale PICs. Compared with time-consuming numerical simulations, we demonstrate that our proposed method is highly efficient in terms of accuracy and computation time: an error rate of smaller than 1% and a speed-up of greater than 100× are achieved. Employing the proposed method, we study 60 identical microresonators (MRs) on a 2.1×4.5 mm^2 chip fabricated by the electron beam lithography system at the university of Washington with a high resolution of 2 nm. Our study quantifies the worst-case within-die silicon thickness variation and resonance wavelength shift to be 1.55 and 2.11 nm, respectively. Moreover, not only do we confirm a strong correlation among the resonance wavelengths of the MRs in proximity as in [1], but also we demonstrate that the same correlation can exist among the MRs which are not in proximity. The proposed method helps evaluate the impact of process variations on the performance of large-scale PICs, determining power penalties required to trim/tune (e.g., thermal tuning) faulty devices in such systems.

2. Theory

It is possible to consider design parameters sweeps (a.k.a. corner analysis) in a numerical simulation (e.g., FDTD simulation) of a photonic device. However, employing such simulations for large-scale PICs is not feasible due to the computation cost. Our novel contribution is to develop a fast and accurate method to study large-scale PICs under random process variations. Considering an extended version of Marcatili's approach [5], we develop an analytical

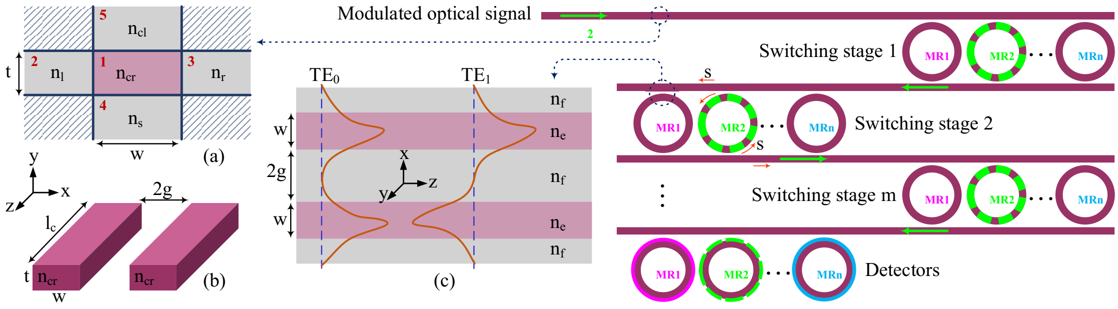

Fig. 1: An illustration of various aspects of a large-scale PIC for WDM-based applications with n wavelengths and m switching stages. All the functional devices utilize MRs, including wavelength-selective photodetectors and photonic switches. (a) 2D approximation of a strip waveguide based on Marcatili's approach; (b) Coupling region in photonic switches; and, (c) 2D approximation of the coupler including the symmetric and antisymmetric supermodes.

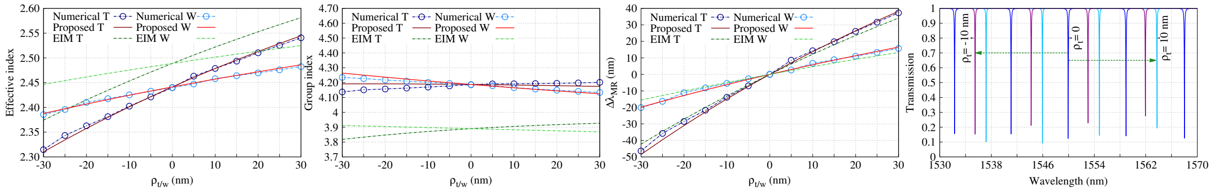

(a) Effective index (b) Group index (c) Resonance wavelength shift (d) Through port response

Fig. 2: Quantitative simulation results of the proposed models, and comparisons with the results from numerical simulations, performed in Lumerical MODE, and the effective index method (EIM). ”T” and ”W” stand for thickness and width variations, respectively. The resonance wavelength shift in (c) is independent of the MR radius. (d) Optical spectrum of our fabricated TE polarization MR calculated using the proposed method with r$=10\ \mu$m, $l_c \simeq 1\ \mu$m, $2g = 200$ nm, and $\lambda^0_{MR} = 1550$ nm under $\rho_t = \pm 10$ nm.

method to study the effective and group indices of the fundamental TE mode in strip waveguides under silicon thickness and waveguide width variations. Applying the developed method, Fig. 1(a) illustrates a 2D approximation of a strip waveguide with a thickness and width of t and w, respectively. The waveguide core, region 1, is silicon with a refractive index of $n_{cr}(\lambda)$, where Sellmeier equation is considered to take into account the the impact of material dispersion. The surrounding regions are all from SiO$_2$ with $n_l = n_r = n_s = n_{cl} = 1.444$, in which the dispersion is ignored as the light is mostly confined in the waveguide core.

Finding a solution to E_z and H_z in region 1 that assumes the electric fields (E_x) to be predominantly polarized in the y-direction to satisfy Maxwell’s equations, we can calculate the effective index of the waveguide as $n_{eff}(T,W,\lambda) = \frac{\lambda}{2\pi}\sqrt{n^2_{cr}(\lambda)k^2_0 - k^2_x(T,W,\lambda) - k^2_y(T,W,\lambda)}$. Here, T and W are the thickness and width of the waveguide under variations and they are equal to $t \pm \rho_t$ and $w \pm \rho_w$, respectively. We define ρ_t and ρ_w to take into account the variations in the silicon thickness and waveguide width, respectively. It is worth mentioning that $\rho_{t/w}$ can be assigned by a random number generator function that respects the mean and standard deviation of the variations measured in different fabrications. k_x and k_y are the spatial frequencies that can be found by solving eigenvalue equations for the TM and TE modes in slab waveguides, and k_0 is the free-space wavenumber. Considering the waveguide and material dispersion, the group index can be defined as $n_g(T,W,\lambda) = n_{eff}(T,W,\lambda) - \lambda\frac{dn_{eff}(T,W,\lambda)}{d\lambda}$.

In this specific study using this method, we look at the resonance wavelength shift in MR-based photonic switches under process variations (see Fig. 1). The MR is on resonance when the round-trip optical phase, ϕ_{rt}, is an integer multiple of 2π, i.e., $\phi_{rt}(T,W,\lambda_{MR}) = \frac{2\pi n_{eff}(T,W,\lambda_{MR})L_{rt}(T,W)}{\lambda_{MR}} = m2\pi$, where L_{rt} is the optical round-trip length that equals $2\pi r(T,W) + 2l_c$. Here, $r(T,W)$ is the MR radius under silicon thickness and width variations and l_c is the coupler length (see Fig. 1(b)). Considering the first-order approximation of the waveguide dispersion (since $\frac{\partial n_{eff}}{\partial\lambda} \neq 0$), we can calculate the resonance wavelength shift as $\Delta\lambda_{MR} = \frac{\Delta_{\rho_{t/w}} n_{eff}\lambda^0_{MR}}{n_g(t,w,\lambda^0_{MR})}$, where λ^0_{MR} is the initial resonance wavelength with no variations, and $\Delta_{\rho_{t/w}} n_{eff}$ is the effective index variations under the thickness and waveguide width variations.

As Fig. 1(b) indicates, the coupling region in MR-based photonic switches consists of two directional couplers (DCs). We consider supermode theory to study the straight-through coefficient, s, and the cross-over coupling coefficient, κ, in a DC (see Fig. 1). We assume a symmetric and lossless coupler, i.e., $\kappa^2 + s^2 = 1$, while the optical losses of the coupler are incorporated into the round trip loss of the entire optical cavity. The effective indices of the first two eigenmodes of the coupled waveguides (TE_0, symmetric, and TE_1, antisymmetric, modes in Fig. 1(c)) determine the coefficients: $\kappa(T,W,\lambda) = \left|sin\left(\frac{[n_{effTE_0}(T,W,\lambda) - n_{effTE_1}(T,W,\lambda)]\pi}{\lambda}l_c\right)\right|$. Here, $n_{effTE_{0/1}}$ can be calculated based on the 2D approximation of the DC indicated in Fig. 1(c) (i.e., a five-layer slab waveguide structure), in which $n_e(\lambda)$ is the effective index of the slab waveguide in the y direction in Fig. 1(b), and n_f=1.444. The optical spectra of the photonic switches under variations can be simply calculated using the methodology presented in this section.

3. Results, Fabrication and Discussion

The quantitative simulation results of the proposed models, performed in MATLAB, are indicated in Fig. 2. We consider strip waveguides with $w = 500$ and $t = 220$ nm (same in our fabrication), and a variation range of $\rho_{t/w} \in$[-30, 30] nm (only in our simulations). Also, the central wavelength, λ, is at 1550 nm. As the figure indicates, compared with the numerical simulation results, our method indicates very high accuracy with an error rate of smaller than 1%. Particularly, our method achieves a speed-up of greater than 100×. Fig. 3(a) illustrates the unit cell of the fabricated